Modelling and Control of a Robotic Hula–hoop System without Velocity Measurements

Alejandro Gutiérrez–Giles, * **Fabio Ruggiero,** *
Vincenzo Lippiello, * **Bruno Siciliano** *

* *Department of Electrical Engineering and Information Technology, University of Naples Federico II, Via Claudio 21, 80125, Naples, Italy, (e-mails: {giles.gutierrez, fabio.ruggiero, vincenzo.lippiello, bruno.siciliano}@unina.it)*

Abstract: The contact kinematics of a robotic hoop and a pole system is obtained by using the Montana's equations, considering the case of contact without slipping. The resulting kinematic model is completely nonholonomic. After some mild assumptions, a set of Pfaffian constraints is established. Then, a dynamic model of the system is developed by employing the Lagrange–d'Alembert formulation. This dynamic model, which represents an underactuated mechanical system, is later used to design a controller which does not need velocity measurements. The proposed method, and its robustness against model uncertainties, is validated through numeric simulations.

Keywords: Mechatronic systems, Motion control systems, Autonomous robotic systems, Modelling

1. INTRODUCTION

When dealing with the problem of a robotic manipulator interacting with an object, most of the works in the literature are devoted to tasks where the object is firstly grasped by the manipulator and then a desired trajectory is followed (*e.g.,* pick–and–place). Alternatively, interaction with objects can be performed without grasping, what is called *nonprehensile manipulation* (Lynch and Mason, 1999). Nonprehensile manipulation enhances the capabilities of a robot inasmuch as it extends the manipulator workspace and, more importantly, the quantity of tasks that can be performed. However, since the number of degrees of freedom is generally increased, both mathematical modelling and analysis can be more complicated than in the prehensile case. To deal with this problem, a complex nonprehensile manipulation task is commonly decomposed in simpler sub–tasks called *primitives*. As mentioned in Lynch and Mason (1999), some examples of such primitives are *sliding, rolling, pushing, throwing, catching*, and so on.

In the rolling primitive context, some study cases are successfully addressed in the literature, *e.g.,* a juggler's *butterfly* movement (Lynch et al., 1998; Surov et al., 2015), a disk–on–a–disk system (Ryu et al., 2013; Donaire et al., 2016b), and a ball rolling on a bowl (Choudhury and Lynch, 2000). The underlying motivation for studying such kind of problems is to make it possible for robotic systems to perform complex tasks, in an attempt to emulate the human capabilities.

In this paper, an example of the rolling nonprehensile manipulation primitive is studied, *i.e.,* a hula–hoop system. This system consists of a pole in contact with a hoop. The pole is intended to be moved for inducing, through contact, a spinning movement of the hoop. There are few works in the literature approaching the robotic hula–hoop. One of the early works (Caughey, 1960) studies the relation between the limit cycles of a pendulum oscillating in a planar movement with the hoop dynamics and its dependence on initial conditions and parameters. In Seyranian and Belyakov (2011) two exact solutions for the hoop movement in an horizontal plane under an open–loop controller action are presented. Some experimental results with a dedicated robot and an open–loop controller are shown in Kakehashi et al. (2012).

In contrast with all the mentioned works, in Nishizaki et al. (2009) a dynamic model and a control strategy are developed to stabilise a pole and a hoop system considering non–planar movement. This is carried out by employing the Montana's equations (Montana, 1988) to obtain the contact kinematics. The authors proposed a partial feedback linearisation controller to stabilise the hoop movement.

In this work, a similar modelling procedure as the described in Nishizaki et al. (2009) is followed. First, the Montana's equations are employed to obtain a kinematic model. This kinematic model can be shown to be *completely nonholonomic* (Siciliano et al., 2010, p. 477). Second, a set of Pffafian constraints are obtained from the kinematic model. Next, the Lagrange–d'Alembert equa-

⋆ This work was partially supported by the RoDyMan project, which has received funding from the European Research Council FP7 Ideas under Advanced Grant agreement number 320992. The authors are solely responsible for the content of this manuscript.

tions are used to obtain a dynamic model satisfying the nonholonomic constraints. As a result, a mechanical system with three inputs and eight generalised coordinates is obtained. A simplification procedure based on the Pffafian constraints can be employed to project the dynamics into the subspace of allowable motions, obtaining a set of five second–order differential equations with two inputs. These equations have a Lagrangian structure with five coordinates and three inputs. The resulting underactuated mechanical system has the property of being *strongly inertially coupled* (Spong, 1994). Also, the constraints are of the *second order* kind (Oriolo and Nakamura, 1991). Regrettably, the conditions given in Olfati-Saber (2000) to transform the model into a *cascade form*, with the subsequent control design simplification, are not satisfied. In addition, the control objective cannot be reduced to a regulation problem, but tracking in the underactuated coordinates must be achieved. This restriction disallows the direct application of the otherwise *ad hoc* result proposed in Donaire et al. (2016a).

Finally, in this paper, an extended–state high–gain observer controller is designed for the reduced model to avoid both velocity measurements and complete dependence on the mathematical model.

2. KINEMATICS

Consider the hoop and a pole system shown in Figure 1. In this figure, the inertial, pole, hoop, and contact Cartesian frames are displayed, corresponding to the subscripts w, p, h, and c, respectively. The contact frame is defined as follows: $\boldsymbol{o}_\mathrm{c}$ is located at the contact point, $\boldsymbol{x}_\mathrm{c}$ is in the line connecting the hoop centre with the contact point and pointing outwards the pole, $\boldsymbol{z}_\mathrm{c}$ is normal to the hoop equatorial plane passing through $\boldsymbol{o}_\mathrm{c}$, and $\boldsymbol{y}_\mathrm{c}$ is chosen to form an orthonormal frame.

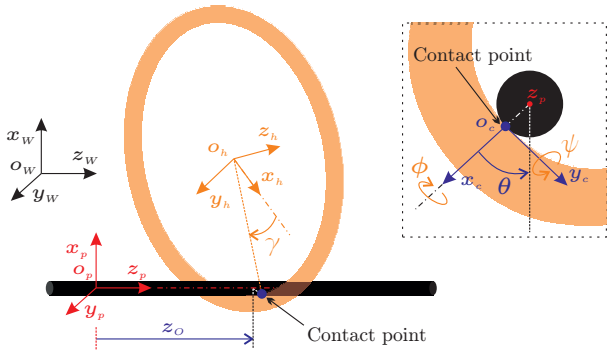

Fig. 1. Pole and hoop system.

The following notation is adopted: $\boldsymbol{v}_i^j$ means that the vector $\boldsymbol{v}_i$ is referred to the j frame. If a vector or matrix is referred to the world coordinate frame the superscript $(\cdot)^\mathrm{w}$ is omitted. The notation $\boldsymbol{I}_n$ is adopted for the $n \times n$ identity matrix and $\boldsymbol{O}_{n\times m}$ for the zero matrix of dimension $n \times m$. For the $m = 1$ case, $\boldsymbol{0}$ denotes the zero vector of dimension n.

2.1 Pole equations

Define the following local coordinates for the pole surface:

- θ: angle from one arbitrarily defined point on the pole surface to the contact point, measured by taking $\boldsymbol{z}_\mathrm{p}$ as the rotation axis.
- z_o: distance form the origin $\boldsymbol{o}_\mathrm{p}$ to the contact point over the $\boldsymbol{z}_\mathrm{p}$ axis.

Let $\boldsymbol{\alpha}_\mathrm{o} \triangleq (\theta, z_\mathrm{o})$, then the pole surface in local coordinates is described by

$$\boldsymbol{c}_\mathrm{o}(\boldsymbol{\alpha}_\mathrm{o}) = [r_\mathrm{p}c_\theta \;\; r_\mathrm{p}s_\theta \;\; z_\mathrm{o}]^\mathrm{T} \,, \tag{1}$$

where r_p is the pole radius, $c_\theta \triangleq \cos(\theta)$, and $s_\theta \triangleq \sin(\theta)$. The tangent vectors are thus computed as

$$\boldsymbol{c}_{\mathrm{o}_\mathrm{u}} = [-r_\mathrm{p}s_\theta \;\; r_\mathrm{p}c_\theta \;\; 0]^\mathrm{T} \tag{2}$$

$$\boldsymbol{c}_{\mathrm{o}_\mathrm{v}} = [0 \;\; 0 \;\; 1]^\mathrm{T} \,. \tag{3}$$

It is easy to see that $\|\boldsymbol{c}_{\mathrm{o}_\mathrm{u}}\| = r_\mathrm{p}$ and $\|\boldsymbol{c}_{\mathrm{o}_\mathrm{v}}\| = 1$. The corresponding normal vector is given by

$$\boldsymbol{n}_\mathrm{o} = [c_\theta \;\; s_\theta \;\; 0]^\mathrm{T} \,, \tag{4}$$

with partial derivatives

$$\boldsymbol{n}_{\mathrm{o}_\mathrm{u}} = [-s_\theta \;\; c_\theta \;\; 0]^\mathrm{T} \tag{5}$$

$$\boldsymbol{n}_{\mathrm{o}_\mathrm{v}} = [0 \;\; 0 \;\; 0]^\mathrm{T} \,. \tag{6}$$

The second–order partial derivatives of $\boldsymbol{c}_{\mathrm{o}_\mathrm{u}}$, necessary to compute the torsion, are

$$\boldsymbol{c}_{\mathrm{o}_{\mathrm{uu}}} = [-r_\mathrm{p}c_\theta \;\; -r_\mathrm{p}s_\theta \;\; 0]^\mathrm{T} \tag{7}$$

$$\boldsymbol{c}_{\mathrm{o}_{\mathrm{uv}}} = [0 \;\; 0 \;\; 0]^\mathrm{T} \,. \tag{8}$$

Therefore, following the definitions given by Montana (1988), the metric $\boldsymbol{M}_\mathrm{o}$, curvature $\boldsymbol{K}_\mathrm{o}$, and torsion $\boldsymbol{T}_\mathrm{o}$ of the pole surface are

$$\boldsymbol{M}_\mathrm{o} = \begin{bmatrix} r_\mathrm{p} & 0 \\ 0 & 1 \end{bmatrix} \,, \quad \boldsymbol{K}_\mathrm{o} = \begin{bmatrix} 1/r_\mathrm{p} & 0 \\ 0 & 0 \end{bmatrix} \,, \quad \boldsymbol{T}_\mathrm{o} = [0 \;\; 0] \,.$$

2.2 Hoop equations

The following local coordinates for the hoop are defined:

- γ: angle from one arbitrarily defined point in the hoop surface to the contact point measured by taking $\boldsymbol{z}_\mathrm{h}$ as the rotation axis.
- ψ: angle of the equatorial plane of the hoop over $\boldsymbol{y}_\mathrm{c}$.

Define $\boldsymbol{\alpha}_\mathrm{f} \triangleq (\gamma, \psi)$, so the hoop surface in local coordinates can be described by

$$\boldsymbol{c}_\mathrm{f}(\boldsymbol{\alpha}_\mathrm{f}) = [-(l_\mathrm{h} - r_\mathrm{h}c_\psi)c_\gamma \;\; (l_\mathrm{h} - r_\mathrm{h}c_\psi)s_\gamma \;\; -r_\mathrm{h}s_\psi]^\mathrm{T} \,, \tag{9}$$

where l_h and $2r_\mathrm{h}$ are the hoop radius and thickness, respectively. The corresponding tangent vectors are computed as

$$\boldsymbol{c}_{\mathrm{f}_\mathrm{u}} = [-(l_\mathrm{h} - r_\mathrm{h}c_\psi)s_\gamma \;\; (l_\mathrm{h} - r_\mathrm{h}c_\psi)c_\gamma \;\; 0]^\mathrm{T} \tag{10}$$

$$\boldsymbol{c}_{\mathrm{f}_\mathrm{v}} = [r_\mathrm{h}c_\gamma s_\psi \;\; r_\mathrm{h}s_\gamma s_\psi \;\; -r_\mathrm{h}c_\psi]^\mathrm{T} \,. \tag{11}$$

In this case, $\|\boldsymbol{c}_{\mathrm{f}_\mathrm{u}}\| = l_\mathrm{h} - r_\mathrm{h}c_\psi$ and $\|\boldsymbol{c}_{\mathrm{f}_\mathrm{v}}\| = r_\mathrm{h}$. The normal vector is given by

$$\boldsymbol{n}_\mathrm{f} = [-c_\gamma c_\psi \;\; -s_\gamma c_\psi \;\; -s_\psi]^\mathrm{T} \,, \tag{12}$$

with partial derivatives

$$\boldsymbol{n}_{\mathrm{f}_\mathrm{u}} = [s_\gamma c_\psi \;\; -c_\gamma c_\psi \;\; 0]^\mathrm{T} \tag{13}$$

$$\boldsymbol{n}_{\mathrm{f}_\mathrm{v}} = [c_\gamma s_\psi \;\; s_\gamma s_\psi \;\; -c_\psi]^\mathrm{T} \,. \tag{14}$$

The second–order partial derivatives of $\boldsymbol{c}_{\mathrm{f}_\mathrm{u}}$ are

$$\boldsymbol{c}_{\mathrm{f}_{\mathrm{uu}}} = [-(l_\mathrm{h} - r_\mathrm{h}c_\psi)c_\gamma \;\; -(l_\mathrm{h} - r_\mathrm{h}c_\psi)s_\gamma \;\; 0]^\mathrm{T} \tag{15}$$

$$\boldsymbol{c}_{\mathrm{f}_{\mathrm{uv}}} = [-r_\mathrm{h}s_\gamma s_\psi \;\; r_\mathrm{h}c_\gamma s_\psi \;\; 0]^\mathrm{T} \,. \tag{16}$$

For the hoop surface, the metric $\boldsymbol{M}_{\mathrm{f}}$, curvature $\boldsymbol{K}_{\mathrm{f}}$, and torsion $\boldsymbol{T}_{\mathrm{f}}$ are given by

$$\boldsymbol{M}_{\mathrm{f}} = \begin{bmatrix} l_{\mathrm{h}} - r_{\mathrm{h}} c_{\psi} & 0 \\ 0 & r_{\mathrm{h}} \end{bmatrix}, \quad \boldsymbol{K}_{\mathrm{f}} = \begin{bmatrix} -c_{\psi} / \left(l_{\mathrm{h}} - r_{\mathrm{h}} c_{\psi}\right) & 0 \\ 0 & 1/r_{\mathrm{h}} \end{bmatrix},$$
$$\boldsymbol{T}_{\mathrm{f}} = \begin{bmatrix} -s_{\psi} / \left(l_{\mathrm{h}} - r_{\mathrm{h}} c_{\psi}\right) & 0 \end{bmatrix}.$$

The fifth coordinate ϕ is the angle form $\boldsymbol{c}_{\mathrm{ou}}$ to $\boldsymbol{c}_{\mathrm{fu}}$, measured over the x_{c} axis. The relative curvature is given by

$$\tilde{\boldsymbol{K}}_{\mathrm{o}} = \frac{1}{r_{\mathrm{p}}} \begin{bmatrix} c_{\phi}^2 & -s_{\phi} c_{\phi} \\ -s_{\phi} c_{\phi} & s_{\phi}^2 \end{bmatrix}. \tag{17}$$

Now, by combining both surface geometric parameters, the Montana's equations in terms of the relative velocities ω_x and ω_y between the contact frames, assuming no sliding, *i.e.,* $v_x = v_y = v_z = \omega_z = 0$ are given by

$$\begin{bmatrix} \dot{\gamma} \\ \dot{\psi} \end{bmatrix} = \frac{1}{l_{\mathrm{h}} c_{\phi}^2 - (r_{\mathrm{p}} + r_{\mathrm{h}}) c_{\psi}} \begin{bmatrix} r_{\mathrm{p}} + r_{\mathrm{h}} s_{\phi}^2 \\ (l_{\mathrm{h}} - r_{\mathrm{h}} c_{\psi}) s_{\phi} c_{\phi} \end{bmatrix}$$
$$\begin{bmatrix} r_{\mathrm{h}} s_{\phi} c_{\phi} \\ (l_{\mathrm{h}} - r_{\mathrm{h}} c_{\psi}) c_{\phi}^2 - r_{\mathrm{p}} c_{\psi} \end{bmatrix} \begin{bmatrix} -\omega_y \\ \omega_x \end{bmatrix} \tag{18}$$

$$\begin{bmatrix} \dot{\theta} \\ \dot{z}_{\mathrm{o}} \end{bmatrix} = \frac{1}{l_{\mathrm{h}} c_{\phi}^2 - (r_{\mathrm{p}} + r_{\mathrm{h}}) c_{\psi}} \begin{bmatrix} (l_{\mathrm{h}} - r_{\mathrm{h}} c_{\psi}) c_{\phi} \\ -(l_{\mathrm{h}} - r_{\mathrm{h}} c_{\psi})(r_{\mathrm{p}} + r_{\mathrm{h}}) s_{\phi} \end{bmatrix}$$
$$\begin{bmatrix} r_{\mathrm{h}} s_{\phi} c_{\psi} \\ -r_{\mathrm{h}} c_{\phi} \left(l_{\mathrm{h}} - (r_{\mathrm{p}} + r_{\mathrm{h}}) c_{\psi}\right) \end{bmatrix} \begin{bmatrix} -\omega_y \\ \omega_x \end{bmatrix} \tag{19}$$

$$\dot{\phi} = \frac{(r_{\mathrm{p}} + r_{\mathrm{h}} s_{\phi}^2) s_{\psi} \omega_y - r_{\mathrm{h}} s_{\phi} c_{\phi} s_{\psi} \omega_x}{l_{\mathrm{h}} c_{\phi}^2 - (r_{\mathrm{p}} + r_{\mathrm{h}}) c_{\psi}}. \tag{20}$$

2.3 Simplifications and Pfaffian constraints

By defining the contact coordinates vector

$$\boldsymbol{q}_{\mathrm{c}} = \left[\gamma \ \psi \ \theta \ z_{\mathrm{o}} \ \phi\right]^{\mathrm{T}}, \tag{21}$$

the kinematic equations (18)–(20) can be rewritten as

$$\dot{\boldsymbol{q}}_{\mathrm{c}} = \boldsymbol{g}_1 \omega_x + \boldsymbol{g}_2 \omega_y, \tag{22}$$

where

$$\boldsymbol{g}_1 = \frac{1}{l_{\mathrm{h}} c_{\phi}^2 - (r_{\mathrm{p}} + r_{\mathrm{h}}) c_{\psi}} \begin{bmatrix} r_{\mathrm{h}} s_{\phi} c_{\phi} \\ (l_{\mathrm{h}} - r_{\mathrm{h}} c_{\psi}) c_{\phi}^2 - r_{\mathrm{p}} c_{\psi} \\ r_{\mathrm{h}} s_{\phi} c_{\psi} \\ -r_{\mathrm{h}} c_{\phi} \left(l_{\mathrm{h}} - (r_{\mathrm{p}} + r_{\mathrm{h}}) c_{\psi}\right) \\ -r_{\mathrm{h}} s_{\phi} c_{\phi} s_{\psi} \end{bmatrix} \tag{23}$$

$$\boldsymbol{g}_2 = \frac{1}{l_{\mathrm{h}} c_{\phi}^2 - (r_{\mathrm{p}} + r_{\mathrm{h}}) c_{\psi}} \begin{bmatrix} -(r_{\mathrm{p}} + r_{\mathrm{h}} s_{\phi}^2) \\ -(l_{\mathrm{h}} - r_{\mathrm{h}} c_{\psi}) s_{\phi} c_{\phi} \\ -(l_{\mathrm{h}} - r_{\mathrm{h}} c_{\psi}) c_{\phi} \\ (l_{\mathrm{h}} - r_{\mathrm{h}} c_{\psi})(r_{\mathrm{p}} + r_{\mathrm{h}}) s_{\phi} \\ (r_{\mathrm{p}} + r_{\mathrm{h}} s_{\phi}^2) s_{\psi} \end{bmatrix}. \tag{24}$$

In order to simplify the kinematic model, assume that the hoop thickness can be neglected, *i.e.,* $r_{\mathrm{h}} = 0$. By choosing a basis for the left null space of $\boldsymbol{G} \triangleq [\boldsymbol{g}_1 \ \boldsymbol{g}_2]$ one can construct a set of Pffafian constraints (Murray et al., 1994, p. 320) given by

$$\boldsymbol{A}_{\mathrm{c}}(\boldsymbol{q}_{\mathrm{c}}) \dot{\boldsymbol{q}}_{\mathrm{c}} = \boldsymbol{0}, \tag{25}$$

where

$$\boldsymbol{A}_{\mathrm{c}}(\boldsymbol{q}_{\mathrm{c}}) = \begin{bmatrix} -l_{\mathrm{h}} c_{\phi} / r_{\mathrm{p}} & 0 & 1 & 0 & 0 \\ s_{\psi} & 0 & 0 & 1 & 0 \\ l_{\mathrm{h}} s_{\phi} & 0 & 0 & 0 & 1 \end{bmatrix}. \tag{26}$$

Let $\boldsymbol{q}_{\mathrm{p}} \triangleq [x_{\mathrm{p}} \ y_{\mathrm{p}} \ z_{\mathrm{p}}]$ be the generalised coordinates of the pole expressing its position in the Cartesian space. Also, define the vectors $\boldsymbol{q}_{\mathrm{r}} \triangleq \left[\gamma \ \psi \ \boldsymbol{q}_{\mathrm{p}}\right]^{\mathrm{T}}$, $\boldsymbol{q}_{\mathrm{s}} \triangleq \left[\theta \ \phi \ z_{\mathrm{o}}\right]^{\mathrm{T}}$, and $\boldsymbol{q} \triangleq \left[\boldsymbol{q}_{\mathrm{r}} \ \boldsymbol{q}_{\mathrm{s}}\right]^{\mathrm{T}}$. Then, the constraints (26) can be written as

$$\boldsymbol{A}_{\mathrm{r}}(\boldsymbol{q}) \dot{\boldsymbol{q}}_{\mathrm{r}} + \dot{\boldsymbol{q}}_{\mathrm{s}} = \boldsymbol{0}, \tag{27}$$

where

$$\boldsymbol{A}_{\mathrm{r}}(\boldsymbol{q}) = \begin{bmatrix} -l_{\mathrm{h}} c_{\phi} / r_{\mathrm{p}} & 0 & 0 & 0 & 0 \\ s_{\psi} & 0 & 0 & 0 & 0 \\ l_{\mathrm{h}} s_{\phi} & 0 & 0 & 0 & 0 \end{bmatrix}. \tag{28}$$

3. DYNAMICS

Let $\boldsymbol{x}_{\mathrm{h}}^{\mathrm{p}} \triangleq \left[x_{\mathrm{h}}^{\mathrm{p}} \ y_{\mathrm{h}}^{\mathrm{p}} \ z_{\mathrm{h}}^{\mathrm{p}}\right]^{\mathrm{T}}$ be the position vector of the hoop centre with respect to the pole frame [1], which in terms of the generalised coordinates is expressed as

$$\boldsymbol{x}_{\mathrm{h}}^{\mathrm{p}} = \begin{bmatrix} -l_{\mathrm{h}} c_{\theta} c_{\psi} + r_{\mathrm{p}} c_{\theta} + l_{\mathrm{h}} s_{\theta} s_{\phi} s_{\psi} \\ r_{\mathrm{p}} s_{\theta} - l_{\mathrm{h}} c_{\psi} s_{\theta} - l_{\mathrm{h}} c_{\theta} s_{\phi} s_{\psi} \\ l_{\mathrm{h}} s_{\psi} + z_{\mathrm{o}} \end{bmatrix}. \tag{29}$$

Notice that, since $\boldsymbol{R}_{\mathrm{p}} = \boldsymbol{I}_3$, it holds $\dot{\boldsymbol{x}}_{\mathrm{h}} = \dot{\boldsymbol{x}}_{\mathrm{h}}^{\mathrm{p}} + \dot{\boldsymbol{q}}_{\mathrm{p}}$. Now, let m_{p} and m_{h} be the hoop and pole masses, respectively, and let g be the gravity acceleration constant. Thus, the system Lagrangian is

$$\mathcal{L}(\boldsymbol{q}, \dot{\boldsymbol{q}}) = \frac{1}{2} m_{\mathrm{h}} \dot{\boldsymbol{x}}_{\mathrm{h}}^{\mathrm{T}} \dot{\boldsymbol{x}}_{\mathrm{h}} + \frac{1}{2} \boldsymbol{\omega}_{\mathrm{h}}^{\mathrm{T}} \boldsymbol{R}_{\mathrm{h}} \mathcal{I}_{\mathrm{h}} \boldsymbol{R}_{\mathrm{h}}^{\mathrm{T}} \boldsymbol{\omega}_{\mathrm{h}}$$
$$+ \frac{1}{2} m_{\mathrm{p}} \dot{\boldsymbol{q}}_{\mathrm{p}}^{\mathrm{T}} \dot{\boldsymbol{q}}_{\mathrm{p}} - m_{\mathrm{h}} g (x_{\mathrm{h}}^{\mathrm{p}} + x_{\mathrm{p}}) - m_{\mathrm{p}} g x_{\mathrm{p}}, \tag{30}$$

where $\mathcal{I}_{\mathrm{h}} = \mathrm{diag}\left\{\frac{1}{2} m_{\mathrm{h}} l_{\mathrm{h}}^2, \frac{1}{2} m_{\mathrm{h}} l_{\mathrm{h}}^2, m_{\mathrm{h}} l_{\mathrm{h}}^2\right\}$ is the hoop inertia tensor with respect to the hoop frame, $\boldsymbol{\omega}_{\mathrm{h}}$ is the hoop angular velocity, and

$$\boldsymbol{R}_{\mathrm{h}} = \begin{bmatrix} c_{\psi} c_{\theta} - s_{\phi} s_{\psi} s_{\theta} & -c_{\phi} s_{\theta} & c_{\theta} s_{\psi} + c_{\psi} s_{\phi} s_{\theta} \\ c_{\theta} s_{\phi} s_{\psi} + c_{\psi} s_{\theta} & c_{\phi} c_{\theta} & -c_{\psi} c_{\theta} s_{\phi} + s_{\psi} s_{\theta} \\ -c_{\phi} s_{\psi} & s_{\phi} & c_{\phi} c_{\psi} \end{bmatrix} \tag{31}$$

is the hoop rotation matrix with respect to the inertial frame. The hoop angular velocity can be obtained from this matrix by means of the expression $\boldsymbol{S}(\boldsymbol{\omega}_{\mathrm{h}}) = \dot{\boldsymbol{R}}_{\mathrm{h}} \boldsymbol{R}_{\mathrm{h}}^{\mathrm{T}}$, where $\boldsymbol{S}(\boldsymbol{\omega}_{\mathrm{h}})$ is a well–known skew symmetric matrix constructed from $\boldsymbol{\omega}_{\mathrm{h}}$. The corresponding angular velocity is

$$\boldsymbol{\omega}_{\mathrm{h}} = \begin{bmatrix} c_{\theta} \dot{\phi} - c_{\phi} s_{\theta} \dot{\psi} \\ s_{\theta} \dot{\phi} + c_{\phi} c_{\theta} \dot{\psi} \\ s_{\phi} \dot{\psi} + \dot{\theta} \end{bmatrix}. \tag{32}$$

The Lagrange–d'Alembert equations, properly absorbing the Pfaffian constraints, are given by

$$\left(\frac{\mathrm{d}}{\mathrm{d}t} \frac{\partial \mathcal{L}}{\partial \dot{\boldsymbol{q}}_{\mathrm{r}}} - \frac{\partial \mathcal{L}}{\partial \boldsymbol{q}_{\mathrm{r}}} - \boldsymbol{\Upsilon}_{\mathrm{r}}\right) - \boldsymbol{A}_{\mathrm{r}}^{\mathrm{T}}(\boldsymbol{q}) \left(\frac{\mathrm{d}}{\mathrm{d}t} \frac{\partial \mathcal{L}}{\partial \dot{\boldsymbol{q}}_{\mathrm{s}}} - \frac{\partial \mathcal{L}}{\partial \boldsymbol{q}_{\mathrm{s}}}\right) = \boldsymbol{0}, \tag{33}$$

where

$$\boldsymbol{\Upsilon}_{\mathrm{r}} \triangleq \begin{bmatrix} \boldsymbol{0}_2 \\ \boldsymbol{u} \end{bmatrix}, \tag{34}$$

with $\boldsymbol{u} \in \mathbb{R}^3$ the vector of generalised forces acting on the pole.

The procedure described by Murray et al. (1994, Ch. 6) can be employed to eliminate $\dot{\boldsymbol{q}}_{\mathrm{s}}$ and $\ddot{\boldsymbol{q}}_{\mathrm{s}}$, which results in the dynamic model

$$\boldsymbol{M}_{\mathrm{h}}(\boldsymbol{q}) \ddot{\boldsymbol{q}}_{\mathrm{h}} + \boldsymbol{c}_{\mathrm{h}}(\boldsymbol{q}, \dot{\boldsymbol{q}}_{\mathrm{h}}) + \boldsymbol{T}_{\mathrm{h}}(\boldsymbol{q}) \ddot{\boldsymbol{q}}_{\mathrm{p}} = \boldsymbol{0} \tag{35a}$$

$$\boldsymbol{M}_{\mathrm{p}}(\boldsymbol{q}) \ddot{\boldsymbol{q}}_{\mathrm{p}} + \boldsymbol{c}_{\mathrm{p}}(\boldsymbol{q}, \dot{\boldsymbol{q}}_{\mathrm{h}}) + \boldsymbol{T}_{\mathrm{h}}^{\mathrm{T}}(\boldsymbol{q}) \ddot{\boldsymbol{q}}_{\mathrm{h}} = \boldsymbol{u}, \tag{35b}$$

[1] There is a slight abuse of notation, since $x_{\mathrm{h}}^{\mathrm{p}}$, $y_{\mathrm{h}}^{\mathrm{p}}$, and $z_{\mathrm{h}}^{\mathrm{p}}$ are scalars. The superscript is kept to avoid confusion with the coordinates of the same point with respect to the spatial frame.

where $\boldsymbol{q}_\mathrm{h} \triangleq [\gamma\ \psi]^\mathrm{T}$. Since $\boldsymbol{M}_\mathrm{p}(\boldsymbol{q})$ is always invertible, one can solve (35b) for $\ddot{\boldsymbol{q}}_\mathrm{p}$ and substitute into (35a) to obtain

$$\boldsymbol{M}_\mathrm{r}(\boldsymbol{q})\ddot{\boldsymbol{q}}_\mathrm{h} + \boldsymbol{c}_\mathrm{r}(\boldsymbol{q}, \dot{\boldsymbol{q}}_\mathrm{h}) = \boldsymbol{T}_\mathrm{r}(\boldsymbol{q})\boldsymbol{u}\,, \tag{36}$$

where

$$\boldsymbol{M}_\mathrm{r}(\boldsymbol{q}) \triangleq \boldsymbol{M}_\mathrm{h}(\boldsymbol{q}) - \boldsymbol{T}_\mathrm{h}(\boldsymbol{q})\boldsymbol{M}_\mathrm{p}^{-1}(\boldsymbol{q})\boldsymbol{T}_\mathrm{h}^\mathrm{T}(\boldsymbol{q}) \tag{37}$$

$$\boldsymbol{c}_\mathrm{r}(\boldsymbol{q}, \dot{\boldsymbol{q}}_\mathrm{h}) \triangleq \boldsymbol{c}_\mathrm{h}(\boldsymbol{q}, \dot{\boldsymbol{q}}_\mathrm{h}) - \boldsymbol{T}_\mathrm{h}(\boldsymbol{q})\boldsymbol{M}_\mathrm{p}^{-1}(\boldsymbol{q})\boldsymbol{c}_\mathrm{p}(\boldsymbol{q}, \dot{\boldsymbol{q}}_\mathrm{h}) \tag{38}$$

$$\boldsymbol{T}_\mathrm{r}(\boldsymbol{q}) \triangleq -\boldsymbol{T}_\mathrm{h}(\boldsymbol{q})\boldsymbol{M}_\mathrm{p}^{-1}(\boldsymbol{q})\,. \tag{39}$$

The dynamic model (36) can be further simplified to obtain

$$\ddot{\boldsymbol{q}}_\mathrm{h} = \boldsymbol{f}(\boldsymbol{q}, \dot{\boldsymbol{q}}_\mathrm{h}) + \boldsymbol{g}(\boldsymbol{q})\boldsymbol{u}\,, \tag{40}$$

with the definitions $\boldsymbol{f}(\boldsymbol{q}, \dot{\boldsymbol{q}}_\mathrm{h}) \triangleq -\boldsymbol{M}_\mathrm{r}^{-1}(\boldsymbol{q})\boldsymbol{c}_\mathrm{r}(\boldsymbol{q}, \dot{\boldsymbol{q}}_\mathrm{h})$, and $\boldsymbol{g}(\boldsymbol{q}) \triangleq \boldsymbol{M}_\mathrm{r}^{-1}(\boldsymbol{q})\boldsymbol{T}_\mathrm{r}(\boldsymbol{q})$.

Remark 1. The main difference of this section with respect to the model presented by Nishizaki et al. (2009) is that the Lagrange–d'Alembert formulation has been directly applied instead of the Euler–Lagrange one. By using the Lagrange–d'Alembert equations, the dynamics of the system is projected on the space of allowable motions, what can be exploited to reduce the number of states. Another difference is that the coupled model, with the full state comprehending the pole and the hoop coordinates, has been considered. □

4. CONTROL

The control objective is to regulate the contact point position to an arbitrary desired value while simultaneously spinning the hoop at a desired angular speed. At the same time, the hoop must remain in the pole transversal plane. More precisely, the control goal can be expressed as driving $\dot{\gamma} \to \dot{\gamma}_\mathrm{d}$ and $(\psi, \theta, z_\mathrm{o}, \phi) \to (0, 0, z_\mathrm{od}, 0)$, with $\dot{\gamma}_\mathrm{d}, z_\mathrm{od}$ desired constants. The control objective can be simplified, assuming $\dot{\gamma}(t) \neq 0, \forall t \geq t_0$, by defining the desired velocity for the ψ coordinate as

$$\dot{\psi}_\mathrm{d} = (-l_\mathrm{h} s_\phi s_\psi^2 - \boldsymbol{k}^\mathrm{T}\boldsymbol{\xi})\dot{\gamma}/(l_\mathrm{h} c_\phi c_\psi)\,, \tag{41}$$

where $\boldsymbol{\xi} \triangleq [\xi_1\ \xi_2\ \xi_3]^\mathrm{T}$, $\xi_1 = z_\mathrm{o} - z_\mathrm{od}$, $\xi_2 = -l_\mathrm{h} s_\phi$, $\xi_3 = l_\mathrm{h} c_\phi s_\psi$, and $\boldsymbol{k} \triangleq [k_1\ k_2\ k_3]^\mathrm{T}$, with $k_1, k_2, k_3 \in \mathbb{R}$ positive constant gains. As stated in Nishizaki et al. (2009), tracking $\dot{\psi} \to \dot{\psi}_\mathrm{d}$, with $\dot{\psi}_\mathrm{d}$ defined as in (41), guarantees convergence of $(\psi, \theta, z_\mathrm{o}, \phi) \to (0, 0, z_\mathrm{od}, 0)$ for $-\pi/2 < \phi, \psi < \pi/2$.

In order to carry out a performance comparison, in the next sections it is first introduced a modified version of the noncollocated partial feedback linearisation (NPFL) proposed in Nishizaki et al. (2009), by considering $\boldsymbol{u}$ as the control input instead of the pole acceleration $\ddot{\boldsymbol{q}}_\mathrm{p}$. Later, the output feedback controller proposed in this work is developed.

4.1 Noncollocated partial feedback linearisation

Given the desired velocities $\dot{\gamma}_\mathrm{d}$ and $\dot{\psi}_\mathrm{d}$ as proposed in the last section, the goal is to stabilise the system (40) by designing a control law for $\boldsymbol{u}$. The NPFL control law is given by

$$\boldsymbol{u} = \boldsymbol{g}^{+}(\boldsymbol{q})\left(-\boldsymbol{f}(\boldsymbol{q}, \dot{\boldsymbol{q}}) - \boldsymbol{K}_\mathrm{r}(\dot{\boldsymbol{q}}_\mathrm{h} - \dot{\boldsymbol{q}}_\mathrm{hd})\right)\,, \tag{42}$$

where $(\cdot)^+$ stands for the right pseudo–inverse, $\boldsymbol{K}_\mathrm{r} \in \mathbb{R}^{2\times 2}$ is a diagonal matrix of positive constant gains, and $\dot{\boldsymbol{q}}_\mathrm{hd} \triangleq \left[\dot{\gamma}_\mathrm{d}\ \dot{\psi}_\mathrm{d}\right]^\mathrm{T}$.

4.2 Extended state high–gain observer

To avoid direct measurements of the generalised coordinates time derivatives, the observer–based controller proposed by Sira-Ramírez et al. (2010) is applied to stabilise the system (40). In order to apply this method, consider the following assumptions.

Assumption 4.1. $\boldsymbol{z}_1(t) \triangleq \boldsymbol{f}(\boldsymbol{q}, \dot{\boldsymbol{q}}_\mathrm{h})$ can be locally modelled as a time–dependent Taylor polynomial plus a vector of residual terms, *i.e.,*

$$\boldsymbol{z}_1(t) = \sum_{i=0}^{p} \boldsymbol{a}_i t^i + \boldsymbol{r}(t)\,, \tag{43}$$

where p is the degree of the Taylor polynomial, $\boldsymbol{a}_i$ are vectors of constant coefficients, and $\boldsymbol{r}(t)$ is a vector of residual terms. □

Assumption 4.2. The vector $\boldsymbol{z}_1$ and at least its first p time derivatives are uniformly absolutely bounded for every trajectory of the system. □

Remark 2. While Assumption 4.1 is easily satisfied locally by any dynamic system, Assumption 4.2 is more restrictive. This last assumption can be relaxed for fully actuated mechanical systems to assume only *existence* of the related derivatives, but not their *a priori* boundedness (see Gutiérrez-Giles and Arteaga-Pérez, 2014, for deatils). It is worth to point out that $p = 1$ in (43) is a common choice in the extended state observers literature (see Guo and Zhao, 2012; Li et al., 2012, for example), along with Assumption 4.2. □

Taking into account Assumptions 4.1 and 4.2, and by defining $\boldsymbol{q}_\mathrm{h1} \triangleq \boldsymbol{q}_\mathrm{h}$ and $\boldsymbol{q}_\mathrm{h2} \triangleq \dot{\boldsymbol{q}}_\mathrm{h}$, the extended state model can be written as

$$\dot{\boldsymbol{q}}_\mathrm{h1} = \boldsymbol{q}_\mathrm{h2} \tag{44}$$

$$\dot{\boldsymbol{q}}_\mathrm{h2} = \boldsymbol{z}_1 + \boldsymbol{g}(\boldsymbol{q})\boldsymbol{u} \tag{45}$$

$$\dot{\boldsymbol{z}}_1 = \boldsymbol{z}_2 \tag{46}$$

$$\vdots$$

$$\dot{\boldsymbol{z}}_{p-1} = \boldsymbol{z}_p \tag{47}$$

$$\dot{\boldsymbol{z}}_p = \boldsymbol{r}^{(p)}(t)\,. \tag{48}$$

Now, by defining $\tilde{\boldsymbol{q}}_\mathrm{h1} \triangleq \boldsymbol{q}_\mathrm{h1} - \hat{\boldsymbol{q}}_\mathrm{h1}$ a linear high–gain observer is proposed as

$$\dot{\hat{\boldsymbol{q}}}_\mathrm{h1} = \hat{\boldsymbol{q}}_\mathrm{h2} + \boldsymbol{\lambda}_{p+1}\tilde{\boldsymbol{q}}_\mathrm{h1} \tag{49}$$

$$\dot{\hat{\boldsymbol{q}}}_\mathrm{h2} = \hat{\boldsymbol{z}}_1 + \boldsymbol{g}(\boldsymbol{q})\boldsymbol{u} + \boldsymbol{\lambda}_p\tilde{\boldsymbol{q}}_\mathrm{h1} \tag{50}$$

$$\dot{\hat{\boldsymbol{z}}}_1 = \hat{\boldsymbol{z}}_2 + \boldsymbol{\lambda}_{p-1}\tilde{\boldsymbol{q}}_\mathrm{h1} \tag{51}$$

$$\vdots$$

$$\dot{\hat{\boldsymbol{z}}}_{p-1} = \hat{\boldsymbol{z}}_p + \boldsymbol{\lambda}_1\tilde{\boldsymbol{q}}_\mathrm{h1} \tag{52}$$

$$\dot{\hat{\boldsymbol{z}}}_p = \boldsymbol{\lambda}_0\tilde{\boldsymbol{q}}_\mathrm{h1}\,. \tag{53}$$

Equation (41) must be modified to avoid the employment of $\dot{\gamma}$, this can be done by defining

$$\dot{\psi}_\mathrm{d} = (-l_\mathrm{h} s_\phi s_\psi^2 - \boldsymbol{k}^\mathrm{T}\boldsymbol{\xi})([1\ 0]\,\hat{\dot{\boldsymbol{q}}}_\mathrm{h1})/(l_\mathrm{h} c_\phi c_\psi)\,. \tag{54}$$

In a similar way, the control law (42) is modified as follows

$$\boldsymbol{u} = \boldsymbol{g}^{+}(+\boldsymbol{q})\left(-\hat{\boldsymbol{z}}_1 - \boldsymbol{K}_{\mathrm{r}}(\dot{\boldsymbol{q}}_{\mathrm{h1}} - \dot{\boldsymbol{q}}_{\mathrm{hd}})\right) . \qquad (55)$$

Remark 3. The controller–observer given by (49)–(53) and (55) is known in the literature as Active Disturbance Rejection Control (ADRC). The ADRC does not need the explicit computation of $\boldsymbol{f}(\boldsymbol{q}, \dot{\boldsymbol{q}}_{\mathrm{h}})$ in contrast with the feedback linearisation approach in (42). This term is instead estimated on line, in an approximate but arbitrarily close manner (see Sira-Ramírez et al., 2010, for details). Another important advantage is that it does not rely on velocity measurements. □

5. SIMULATION RESULTS

5.1 Controllers' comparison

Both controllers presented in Section 4 are tested by means of a numeric simulation. The system parameters considered for carrying out the simulations are listed in Table 1.

Table 1. Simulation parameters

Meaning	Parameter	Value
Hoop mass	m_{h}	0.5 kg
Pole mass	m_{p}	10 kg
Hoop radius	l_{h}	0.5 m
Pole radius	r_{p}	0.05 m
Gravity constant	g	9.81 m/s^2

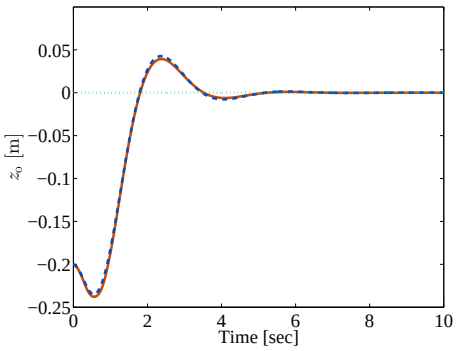

Fig. 2. Contact point position over the pole: NPFL (- - -), ADRC (—), reference (· · ·).

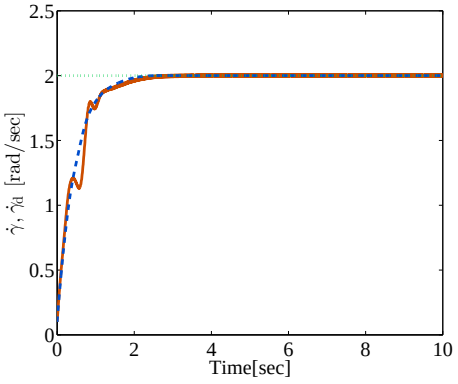

Fig. 3. Hoop angular speed: NPFL (- - -), ADRC (—), reference (· · ·).

For both controllers, the gains in (41)–(42) and (54)–(55) are chosen as $k_1 = k_2 = k_3 = 10$, and $\boldsymbol{K}_{\mathrm{r}} = \mathrm{diag}\{2, 10\}$.

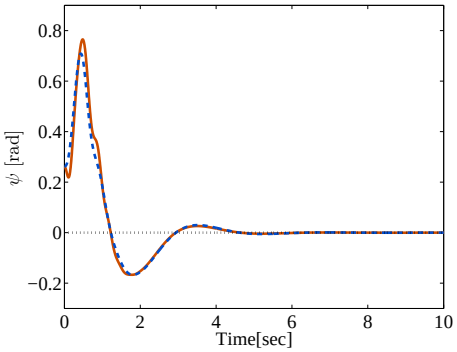

Fig. 4. ψ coordinate: NPFL (- - -), ADRC (—).

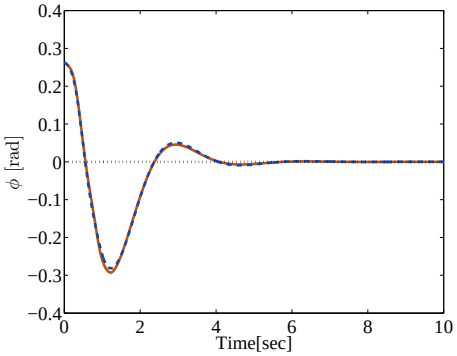

Fig. 5. ϕ coordinate: NPFL (- - -), ADRC (—).

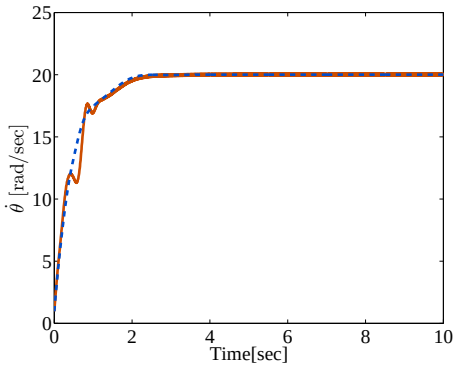

Fig. 6. Velocity $\dot{\theta}$: NPFL (- - -), ADRC (—).

The sampling time for the control loop is set to $T = 0.005\,\mathrm{s}$. It is considered that the state $\boldsymbol{q}$ can be measured by means of a generic sensors system *i.e.,* a vision system. It is also considered that the vision loop acquisition and processing frequency is 50 Hz, *i.e.,* the sample time for this loop is set to $T_{\mathrm{v}} = 0.02\,\mathrm{s}$. The velocities required for the inverse dynamics control are in turn estimated from vision measurements.

For the high–gain observer in Section 4.2 it is chosen $p = 2$, and the gains in (49)–(53) are chosen as $\boldsymbol{\lambda}_0 = 1.6 \times 10^5 \boldsymbol{I}_2$, $\boldsymbol{\lambda}_1 = 3.2 \times 10^4 \boldsymbol{I}_2$, $\boldsymbol{\lambda}_2 = 2.4 \times 10^3 \boldsymbol{I}_2$, and $\boldsymbol{\lambda}_3 = 80 \boldsymbol{I}_2$, *i.e.,* the observer poles are located at $p_1 = p_2 = p_3 = p_4 = -20$.

The initial conditions for the state $\boldsymbol{q}$ in (21) are chosen as $\psi(t_0) = \pi/12\,\mathrm{rad}$, $\gamma(t_0) = \pi/8\,\mathrm{rad}$, $\theta(t_0) = \pi/8\,\mathrm{rad}$, $\phi(t_0) = \pi/12\,\mathrm{rad}$, $z_{\mathrm{o}}(t_0) = -0.2\,\mathrm{m}$, and $x_{\mathrm{p}}(t_0) = y_{\mathrm{p}}(t_0) = z_{\mathrm{p}}(t_0) = 0\,\mathrm{m}$. The initial conditions for all the time

derivatives of the states are set to zero, except for $\dot{\gamma}(t_0) = 0.1\,\text{rad/s}$ and $\dot{\theta}(t_0) = (l_\text{h}/r_\text{p})\,\dot{\gamma}(t_0)$.

The contact point position and the hoop speed time evolution are shown in Figures 2 and 3, respectively. From these figures, it can be seen that the performance is almost the same for both controllers, besides the ADRC needs neither velocity measurements nor the explicit computation of $\boldsymbol{f}(\boldsymbol{q}, \dot{\boldsymbol{q}}_\text{h})$ in (40).

The ψ and ϕ coordinates time evolution is shown in Figures 4 and 5, respectively. Both coordinates ψ and ϕ are driven to zero, which means that the hoop remains in an orthogonal plane with respect to the pole. Finally, in Figure 6 the velocity $\dot{\theta}$ is displayed, where its close relation to $\dot{\gamma}$ in steady state is made evident.

5.2 Robustness test

To test the ADRC controller robustness against uncertainties, the mass of both the hoop and the pole, necessary to compute $\boldsymbol{g}(\boldsymbol{q})$, are varied for the controller implementation in (49)–(53) and (55). The estimated values for the hoop and pole masses are set to 1 kg and 7.5 kg, *i.e.,* 100% and 25% of uncertainty error, respectively.

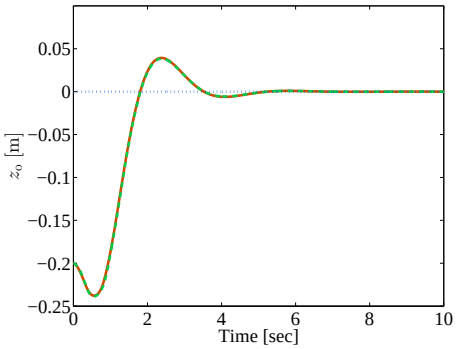

Fig. 7. Contact point position over the pole: nominal (—), uncertain (- - -), reference (· · ·).

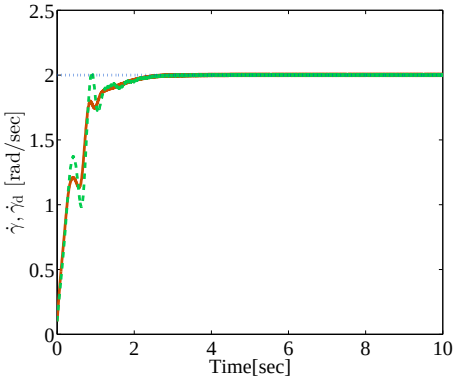

Fig. 8. Hoop angular speed: nominal (—), uncertain (- - -), reference (· · ·).

The contact point position and the angular speed of the hoop around the pole for this case are shown in Figures 7 and 8, respectively. From these figures one can conclude that the performance is not considerably deteriorated despite the uncertainties. The ψ and ϕ coordinates are displayed in Figures 9 and 10, respectively. In Figure 11,

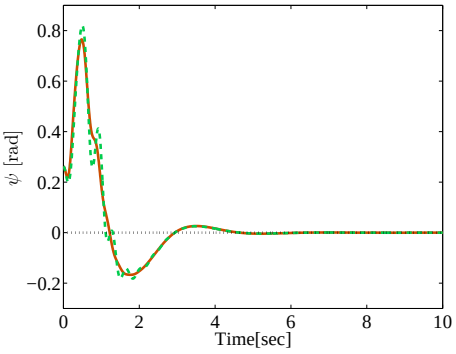

Fig. 9. ψ coordinate: nominal (—), uncertain (- - -).

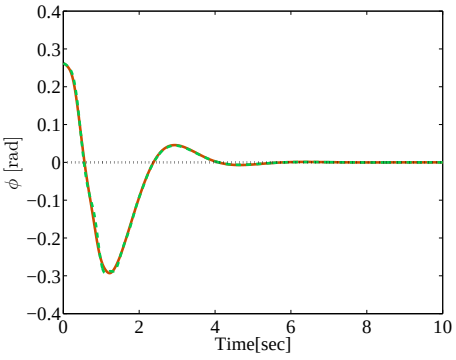

Fig. 10. ϕ coordinate: nominal (—), uncertain (- - -).

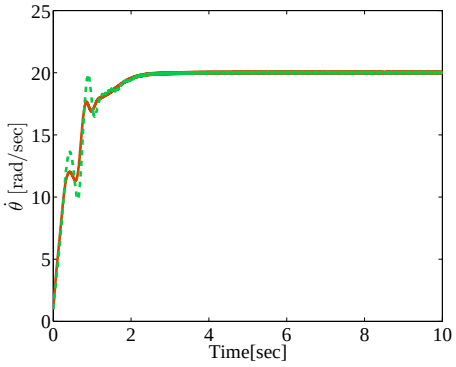

Fig. 11. Velocity $\dot{\theta}$: nominal (—), uncertain (- - -).

the angular velocity of the contact point around the pole is shown. Once again, it can be concluded that the controller performance does not decrease with the uncertainty considered.

5.3 Zero dynamics

Although the hoop is stabilised at a desired spinning velocity and position, the pole position diverges, as pointed out by Nishizaki et al. (2009). This can be seen by analysing the zero dynamics, as proposed by Spong (1994). Whenever the invariant manifold $\boldsymbol{z} = \dot{\boldsymbol{q}}_\text{h} - \dot{\boldsymbol{q}}_\text{hd} = \boldsymbol{0}$ is reached, $\ddot{\boldsymbol{q}}_\text{h} \equiv \boldsymbol{0}$, and the dynamic behaviour of the pole coordinates is described by

$$\ddot{\boldsymbol{q}}_{\mathrm{p}} = -\boldsymbol{M}_{\mathrm{p}}^{-1}\boldsymbol{c}_{\mathrm{p}} - \boldsymbol{T}_{\mathrm{h}}^{+}\boldsymbol{c}_{\mathrm{r}} = \begin{bmatrix} -\dfrac{m_{\mathrm{h}}\omega_{\mathrm{d}}^2(l_{\mathrm{h}}-r_{\mathrm{p}})\cos(\omega_{\mathrm{d}}t) + gm_{\mathrm{s}}\sin^2(\omega_{\mathrm{d}}t)}{m_{\mathrm{s}}} \\ -\dfrac{\left(m_{\mathrm{h}}\omega_{\mathrm{d}}^2(l_{\mathrm{h}}-r_{\mathrm{p}}) + m_{\mathrm{p}}g\cos(\omega_{\mathrm{d}}t)\right)\sin(\omega_{\mathrm{d}}t)}{m_{\mathrm{s}}} \\ 0 \end{bmatrix}, \tag{56}$$

where $m_{\mathrm{s}} = m_{\mathrm{p}} + m_{\mathrm{h}}$, and $\omega_{\mathrm{d}} = (l_{\mathrm{h}}/r_{\mathrm{p}})\dot{\gamma}_{\mathrm{d}}$. The solution of this equation is

$$\boldsymbol{q}_{\mathrm{p}}(t) = \begin{bmatrix} c_1\cos(\omega_{\mathrm{d}}t) + c_2\cos(2\omega_{\mathrm{d}}t) + c_3t^2 + c_4t + c_5 \\ c_6\sin(\omega_{\mathrm{d}}t) + c_7\sin(2\omega_{\mathrm{d}}t) + c_8t + c_9 \\ \dot{z}_{\mathrm{p}}(t_{\mathrm{ss}})t + z_{\mathrm{p}}(t_{\mathrm{ss}}) \end{bmatrix}, \tag{57}$$

where the c_i are suitable integration constants and t_{ss} is the stationary state response time. It can be seen that the pole coordinates trajectories (57) grow unbounded.

6. CONCLUSIONS AND FUTURE WORK

In this work, the model of a robotic hula–hoop system is analysed and improved with respect to the models and controllers currently available in the literature. Additionally, a control strategy that does not depend on velocity measurements nor the full model of the system is proposed. The validity of the approach is tested and compared with a previously reported one by means of numeric simulations.

As a future work, the main challenge is to stabilise the Cartesian position of the pole to avoid its divergence. The dynamic model controllability will be also studied to get an understanding of what its limitations are. The assumptions of maintaining contact and rolling without slipping have to be assured by computing the contact force and the friction cone, given a dry friction coefficient for the pole and hoop specific materials. Finally, a real–time implementation in an experimental platform will be pursued.

REFERENCES

Caughey, T.K. (1960). Hula-hoop: an example of heteroparametric excitation. *American journal of Physics*, 28(2), 104–109.

Choudhury, P. and Lynch, K.M. (2000). Controllability of single input rolling manipulation. In *Robotics and Automation, 2000. Proceedings. ICRA'00. IEEE International Conference on*, volume 1, 354–360. IEEE.

Donaire, A., Mehra, R., Ortega, R., Satpute, S., Romero, J.G., Kazi, F., and Singh, N.M. (2016a). Shaping the energy of mechanical systems without solving partial differential equations. *IEEE Transactions on Automatic Control*, 61(4), 1051–1056.

Donaire, A., Ruggiero, F., Buonocore, L.R., Lippiello, V., and Siciliano, B. (2016b). Passivity-based control for a rolling-balancing system: The nonprehensile disk-on-disk. *IEEE Transactions on Control Systems Technology*.

Guo, B.Z. and Zhao, Z.L. (2012). On convergence of nonlinear extended state observer for multi-input multi-output systems with uncertainty. *IET Control Theory & Applications*, 6(15), 2375–2386.

Gutiérrez-Giles, A. and Arteaga-Pérez, M.A. (2014). Gpi based velocity/force observer design for robot manipulators. *ISA transactions*, 53(4), 929–938.

Kakehashi, Y., Izawa, T., Shirai, T., Nakanishi, Y., Okada, K., and Inaba, M. (2012). Achievement of hula hooping by robots through deriving principle structure towards flexible spinal motion. *Journal of Robotics and Mechatronics*, 24, 540.

Li, S., Yang, J., Chen, W.H., and Chen, X. (2012). Generalized extended state observer based control for systems with mismatched uncertainties. *IEEE Transactions on Industrial Electronics*, 59(12), 4792–4802.

Lynch, K.M. and Mason, M.T. (1999). Dynamic nonprehensile manipulation: Controllability, planning, and experiments. *The International Journal of Robotics Research*, 18(1), 64–92.

Lynch, K.M., Shiroma, N., Arai, H., and Tanie, K. (1998). The roles of shape and motion in dynamic manipulation: The butterfly example. In *Robotics and Automation, 1998. Proceedings. 1998 IEEE International Conference on*, volume 3, 1958–1963. IEEE.

Montana, D.J. (1988). The kinematics of contact and grasp. *The International Journal of Robotics Research*, 7(3), 17–32.

Murray, R.M., Li, Z., Sastry, S.S., and Sastry, S.S. (1994). *A mathematical introduction to robotic manipulation*. CRC press.

Nishizaki, J., Nakaura, S., and Sampei, M. (2009). Modeling and control of hula-hoop system. In *Decision and Control, 2009 held jointly with the 2009 28th Chinese Control Conference. CDC/CCC 2009. Proceedings of the 48th IEEE Conference on*, 4125–4130. IEEE.

Olfati-Saber, R. (2000). Cascade normal forms for underactuated mechanical systems. In *Decision and Control, 2000. Proceedings of the 39th IEEE Conference on*, volume 3, 2162–2167. IEEE.

Oriolo, G. and Nakamura, Y. (1991). Control of mechanical systems with second-order nonholonomic constraints: Underactuated manipulators. In *Decision and Control, 1991., Proceedings of the 30th IEEE Conference on*, 2398–2403. IEEE.

Ryu, J.C., Ruggiero, F., and Lynch, K.M. (2013). Control of nonprehensile rolling manipulation: Balancing a disk on a disk. *IEEE Transactions on Robotics*, 29(5), 1152–1161.

Seyranian, A.P. and Belyakov, A.O. (2011). How to twirl a hula hoop. *American Journal of Physics*, 79(7), 712–715.

Siciliano, B., Sciavicco, L., Villani, L., and Oriolo, G. (2010). Robotics: modelling, planning and control.

Sira-Ramírez, H., Ramírez-Neria, M., et al. (2010). On the linear control of nonlinear mechanical systems. In *Decision and Control (CDC), 2010 49th IEEE Conference on*, 1999–2004. IEEE.

Spong, M.W. (1994). Partial feedback linearization of underactuated mechanical systems. In *Intelligent Robots and Systems' 94.'Advanced Robotic Systems and the Real World', IROS'94. Proceedings of the IEEE/RSJ/GI International Conference on*, volume 1, 314–321. IEEE.

Surov, M., Shiriaev, A., Freidovich, L., Gusev, S., and Paramonov, L. (2015). Case study in non-prehensile manipulation: planning and orbital stabilization of one-directional rollings for the butterfly robot. In *Robotics and Automation (ICRA), 2015 IEEE International Conference on*, 1484–1489. IEEE.